

for patients who fail high dose chemoradiotherapy and autologous stem cell rescue for relapsed and primary refractory Hodgkin lymphoma. *British Journal of Haematology*, **146**, 158–163.

Moskowitz, A.J., Hamlin, P.A., Perales, M.A., Gerecitano, J., Horwitz, S.M., Matasar, M.J., Noy, A., Palomba, M.L., Portlock, C.S., Straus, D.J., Graustein, T., Zelenetz, A.D. & Moskowitz, C.H. (2013) Phase II study of bendamustine in

relapsed and refractory Hodgkin lymphoma. *Journal of Clinical Oncology*, **31**, 456–460.

Younes, A., Oki, Y., Bociek, R.G., Kuruvilla, J., Fanale, M., Neelapu, S., Copeland, A., Buglio, D., Galal, A., Besterman, J., Li, Z., Drouin, M., Patterson, T., Ward, M.R., Paulus, J.K., Ji, Y., Medeiros, L.J. & Martell, R.E. (2011) Mocetinostat for relapsed classical Hodgkin's lymphoma: an open-label, single-arm, phase 2 trial. *The Lancet Oncology*, **12**, 1222–1228.

Zinzani, P.L., Viviani, S., Anastasia, A., Vitolo, U., Luminari, S., Zaja, F., Corradini, P., Spina, M., Brusamolino, E., Gianni, A.M., Santoro, A., Botto, B., Derenzini, E., Pellegrini, C. & Argani, L. (2013) Brentuximab vedotin in relapsed/refractory Hodgkin's lymphoma: Italian experience and results of the use in the daily clinic outside clinical trials. *Haematologica*, **98**, 1232–1236.

## Loss of CCR4 antigen expression after mogamulizumab therapy in a case of adult T-cell leukaemia-lymphoma

Adult T-cell leukaemia-lymphoma (ATL) is an aggressive peripheral T-cell neoplasm caused by human T-cell leukaemia virus type I infection. Most cases of aggressive ATL (acute, lymphoma, or unfavourable chronic type) are resistant to conventional chemotherapeutic agents, and, thus, it has a poor prognosis (Shimoyama, 1991; Tsukasaki *et al*, 2007). Therefore, development of alternative treatment strategies is an urgent issue. CC chemokine receptor 4 (CCR4) is expressed on most ATL cells and has been shown to be a new molecular target of immunotherapy *in vivo* (Ito *et al*, 2009). Mogamulizumab, a novel molecular targeting agent, is a humanized anti-CCR4 immunoglobulin G1 monoclonal antibody with a defucosylated Fc region, and 50% efficacy has been shown as a single agent in a phase II study for relapsed and refractory ATL (Ishida *et al*, 2012). We have little experience with this agent, as large-scale clinical studies have not been conducted. Here, we report an acute ATL case whose tumour cells lost CCR4 expression after administration of mogamulizumab.

A 63-year-old female was admitted to our hospital for fatigue, fever, skin eruption and hypercalcaemia, and was diagnosed with acute-type ATL. We started a dose-intensified chemotherapy of VCAP-AMP-VECP (vincristine, cyclophosphamide, doxorubicin, and prednisone; doxorubicin, rami-mustine, and prednisone; and vindesine, etoposide, carboplatin, and prednisone) immediately. Six cycles were carried out, and partial remission was obtained, but the ATL cells remained in peripheral blood and skin lesions. ATL recurred with skin lesions immediately while myelosuppression was prolonged. Therefore, we started administration of mogamulizumab as a single agent, once per week for 8 weeks at a dose of 1.0 mg/kg. By the end of the treatment, complete remission was obtained with disappearance of ATL cells in peripheral blood, skin lesions, and normalization of lactate dehydrogenase levels. Unfortunately, a similar eruption developed approximately 3 months later, and the ATL relapsed. The patient again underwent mogamulizumab therapy, as she did not want further chemotherapy. However, the

second administration had no effect, and the patient died due to disease progression.

We analysed CCR4 expression on patient ATL cells using multi-colour flow cytometry analysis, as described previously (Tian *et al*, 2011) to reveal the resistance mechanism. After dead cells (propidium iodide positive) and monocytes ( $CD4^{dim} CD14^{+}$ ) were gated out, a CD3 vs. CD7 plot of  $CD4^{dim}/CD7^{low}$  subpopulation, in which ATL cells were highly enriched, was analysed. This analysis clearly revealed loss of CCR4 expression on ATL tumour cells after mogamulizumab therapy (Fig 1). Furthermore, we conducted clonal analysis by

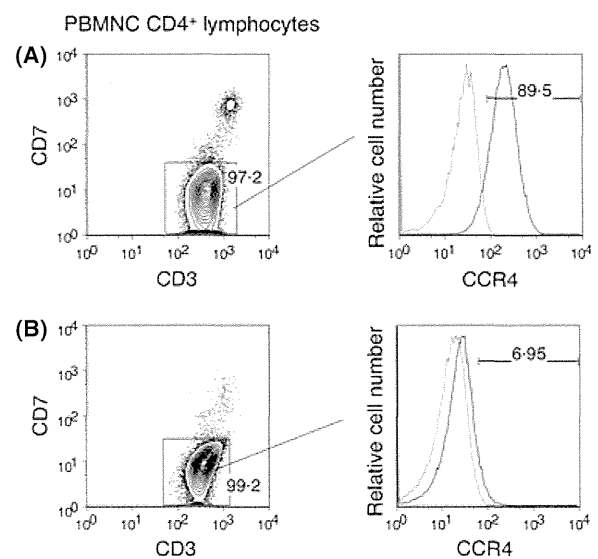


Fig 1. Multicolour flow cytometric analysis of CCR4 expression on adult T-cell leukaemia-lymphoma (ATL) cells. (A) Before mogamulizumab therapy. (B) After second mogamulizumab therapy. The ATL cells accumulated a  $CD7^{low}$  subpopulation before and after treatment, without any change. Loss of the CC chemokine receptor 4 (CCR4) antigen was clearly observed after treatment. PBMNC, peripheral blood mononuclear cells.

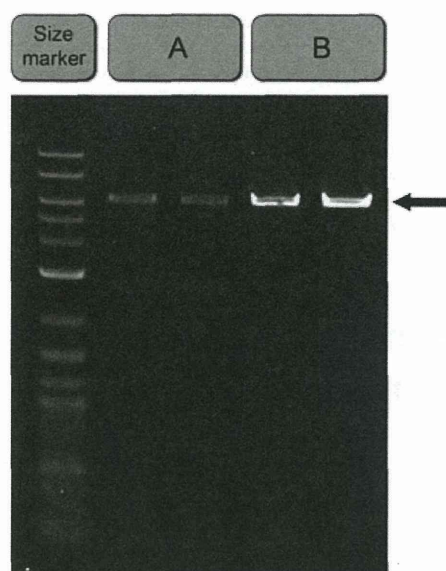


Fig 2. Clonal analysis by inverse long polymerase chain reaction (duplicated). (A) Before mogamulizumab therapy. (B) After second mogamulizumab therapy. The same monoclonal bands were observed before and after mogamulizumab therapy (arrow).

inverse long polymerase chain reaction (PCR) using the same sample. Genomic DNA extracted from peripheral blood mononuclear cells was digested with PstI. The purified DNA was self-ligated with T4 DNA ligase (Takara Bio, Otsu, Japan) and inverse long PCR was performed using Tks Gflex DNA Polymerase (Takara Bio) (Kobayashi *et al*, 2013). The PCRs were performed in duplicate. The band of the major clone was of identical size before and after mogamulizumab therapy (Fig 2), suggesting that the relapsed CCR4<sup>-</sup> ATL cells belonged to the same clone as the original CCR4<sup>+</sup> ATL cells.

To the best of our knowledge, this is the first report of loss of the CCR4 antigen by clonal analysis after mogamulizumab therapy. The resistance mechanism to mogamulizumab has not been elucidated to date. Mogamulizumab exerts its activity on CCR4-expressing T cells through an indirect effector mechanism, antibody-dependent cell-mediated cytotoxicity (ADCC) (Ishii *et al*, 2010). Thus, the CCR4 molecule itself could be involved in the resistance to mogamulizumab by loss of expression. It is believed that target molecular loss is not a rare phenomenon during monoclonal antibody therapy. For example, several reports are available regarding the loss of CD20 expression after the administration of rituximab, which is an anti-CD20 monoclonal antibody (Duman *et al*, 2012). Several mechanisms ranging from the gene to the protein level have been proposed to explain loss of CD20; a similar mechanism might cause loss of CCR4 expression. We demonstrated loss of CCR4 expression on the same ATL clone, which excluded the possibility of a clonal change by CCR4<sup>-</sup> ATL cells after mogamulizumab treatment. We have experienced another

patient who became resistant to a second mogamulizumab administration but whose ATL cells maintained CCR4 expression. Loss of CCR4 expression is one of the resistance mechanisms to mogamulizumab; others include mutation or deletion within epitope-coding regions for mogamulizumab, increase in soluble CCR4, and reduced ADCC.

The anti-CCR4 antibody used in this study, clone 1G1, recognizes a distinct epitope from mogamulizumab (Ishii *et al*, 2010), which excluded the possibility of epitope masking by mogamulizumab. Our results indicate that CCR4 expression by ATL cells should be re-evaluated when relapsed patients with ATL are treated after mogamulizumab therapy even if their tumour cells express CCR4 at the initial evaluation.

### Acknowledgements

We thank Ms. Eri Watanabe (Institute of Medical Science, The University of Tokyo) for technical assistance with flow cytometry. We are grateful to the hospital staff who are committed to providing high-quality care for all of our patients.

### Author contributions

NO and KU wrote the manuscript. SK and TI performed the experiments using patient samples. KY, MK, and KS provided patient care and clinical information. NW supervised the flow cytometry. NO, AT, and KU supervised the research; and all authors approved the final manuscript.

### Conflict of interest

The authors declare no financial conflict of interest.

**Nobuhiro Ohno**<sup>1</sup>  
**Seiichiro Kobayashi**<sup>2</sup>  
**Tomohiro Ishigaki**<sup>2</sup>  
**Koichiro Yuji**<sup>1</sup>  
**Masayuki Kobayashi**<sup>2</sup>  
**Koota Sato**<sup>2</sup>  
**Nobukazu Watanabe**<sup>3</sup>  
**Arinobu Tojo**<sup>1,2</sup>  
**Kaoru Uchimaru**<sup>1</sup>

<sup>1</sup>Department of Haematology/Oncology, Research Hospital, The Institute of Medical Science, The University of Tokyo, <sup>2</sup>Division of Molecular Therapy, The Institute of Medical Science, The University of Tokyo, and <sup>3</sup>Laboratory of Diagnostic Medicine, Division of Stem Cell Therapy, The Institute of Medical Science, The University of Tokyo, Tokyo, Japan  
 E-mail: nobuohno@ims.u-tokyo.ac.jp

**Keywords:** adult T-cell leukaemia-lymphoma, mogamulizumab, CCR4, chemokine receptor 4, monoclonal antibody, flow cytometry

First published online 3 September 2013

doi: 10.1111/bjh.12555

## References

- Duman, B.B., Sahin, B., Ergin, M. & Guvenc, B. (2012) Loss of CD20 antigen expression after rituximab therapy of CD20 positive B cell lymphoma (diffuse large B cell extranodal marginal zone lymphoma combination): a case report and review of the literature. *Medical Oncology*, **29**, 1223–1226.
- Ishida, T., Joh, T., Uike, N., Yamamoto, K., Utsunomiya, A., Yoshida, S., Saburi, Y., Miyamoto, T., Takemoto, S., Suzushima, H., Tsukasaki, K., Nosaka, K., Fujiwara, H., Ishitsuka, K., Inagaki, H., Ogura, M., Akinaga, S., Tomonaga, M., Tobinai, K. & Ueda, R. (2012) Defucosylated anti-CCR4 monoclonal antibody (KW-0761) for relapsed adult T-cell leukemia-lymphoma: a multicenter phase II study. *Journal of Clinical Oncology*, **30**, 837–842.
- Ishii, T., Ishida, T., Utsunomiya, A., Inagaki, A., Yano, H., Komatsu, H., Iida, S., Imada, K., Uchiyama, T., Akinaga, S., Shitara, K. & Ueda, R. (2010) Defucosylated humanized anti-CCR4 monoclonal antibody KW-0761 as a novel immunotherapeutic agent for adult T-cell leukemia/lymphoma. *Clinical Cancer Research*, **16**, 1520–1531.
- Ito, A., Ishida, T., Utsunomiya, A., Sato, F., Mori, F., Yano, H., Inagaki, A., Suzuki, S., Takino, H., Ri, M., Kusumoto, S., Komatsu, H., Iida, S., Inagaki, H. & Ueda, R. (2009) Defucosylated anti-CCR4 monoclonal antibody exerts potent ADCC against primary ATLL cells mediated by autologous human immune cells in NOD/Shi-scid, IL-2R gamma(null) mice in vivo. *Journal of Immunology*, **183**, 4782–4791.
- Kobayashi, S., Tian, Y., Ohno, N., Yuji, K., Ishigaki, T., Isobe, M., Tsuda, M., Oyaizu, N., Watanabe, E., Watanabe, N., Tani, K., Tojo, A. & Uchimaru, K. (2013) The CD3 versus CD7 plot in multicolor flow cytometry reflects progression of disease stage in patients infected with HTLV-I. *PLoS ONE*, **8**, 1–9.
- Shimoyama, M. (1991) Diagnostic criteria and classification of clinical subtypes of adult T-cell leukaemia lymphoma. A report from the Lymphoma Study Group (1984–87). *British Journal of Haematology*, **79**, 428–437.
- Tian, Y., Kobayashi, S., Ohno, N., Isobe, M., Tsuda, M., Zaike, Y., Watanabe, N., Tani, K., Tojo, A. & Uchimaru, K. (2011) Leukemic T cells are specifically enriched in a unique CD3(dim) CD7 (low) subpopulation of CD4(+) T cells in acute-type adult T-cell leukemia. *Cancer science*, **102**, 569–577.
- Tsukasaki, K., Utsunomiya, A., Fukuda, H., Shibata, T., Fukushima, T., Takatsuka, Y., Ikeda, S., Masuda, M., Nagoshi, H., Ueda, R., Tamura, K., Sano, M., Momita, S., Yamaguchi, K., Kawano, F., Hanada, S., Tobinai, K., Shimoyama, M., Hotta, T., Tomonaga, M. & Japan Clinical Oncology Group Study JCOG9801. (2007) VCAP-AMP-VECP compared with biweekly CHOP for adult T-cell leukemia-lymphoma: Japan Clinical Oncology Group Study JCOG9801. *Journal of Clinical Oncology*, **25**, 5458–5464.

## Correlating prothrombin time with plasma rivaroxaban level

Recently published guidelines from the British Committee for Standards in Haematology suggest that the prothrombin time (PT) can be used for urgent determination of anticoagulation intensity with rivaroxaban if a reagent with a known sensitivity is used (Baglin *et al*, 2012). However, it has been established in experiments using normal plasma spiked with varying concentrations of rivaroxaban that different PT reagents may have very different sensitivities to rivaroxaban (Samama *et al*, 2010; Douxfils *et al*, 2012). The clinical implications of this variation in PT sensitivity to rivaroxaban is evident from the recent report by Van Veen *et al* (2013), who described normal PTs in the presence of therapeutic rivaroxaban levels in a patient with renal impairment. Comparing the PT using Innovin<sup>®</sup> (Siemens, Marburg, Germany) and Thromborel S<sup>®</sup> (Siemens) in a patient commenced on rivaroxaban 15 mg twice daily for deep vein thrombosis against the rivaroxaban plasma concentration measured by the Biophen DiXal anti-Xa assay, they demonstrated normal PT results despite therapeutic plasma rivaroxaban levels. They concluded that PT results should be interpreted with caution when assessing coagulation intensity for patients on rivaroxaban (Van Veen *et al*, 2013). If available, a specific anti-Xa assay should be used for patients presenting with major bleeding or when requiring emergency surgery. Mueck *et al* (2011) have also demonstrated variation using Neoplastine<sup>®</sup> (Diagnostica Stago, Asnieres-sur-Seine, France) to measure the PT against rivaroxaban concentration.

However, many coagulation laboratories will not have 24-h access to a rivaroxaban-calibrated anti-Xa assay and will

inevitably rely on their routine coagulation screen PT and activated partial thromboplastin time (APTT) results. Therefore it is essential that laboratories have knowledge of their reagents sensitivity to rivaroxaban. We studied the correlation between the rivaroxaban concentration (measured by Liquid Anti-Xa chromogenic assay, (Instrumentation Laboratory Company, Bedford, MA, USA) run on an IL TOP 700) and PT and APTT. The anti-Xa assay was calibrated using lyophilized standard rivaroxaban plasmas (Hyphen Biomed, Neuville-sur-Oise, France) to create a rivaroxaban assay linear between 0 and 400 ng/ml. Peak rivaroxaban plasma concentrations are considered to be in the range of 100–400 ng/ml, and trough concentrations in the range of 20–150 ng/ml (Baglin *et al*, 2012). PT (Recombiplastin 2G<sup>®</sup>, Instrumentation Laboratory Company, laboratory reference range 9–13 s) and APTT (Synthasil<sup>®</sup>, Instrumentation Laboratory Company, laboratory reference range 27–38 s) were determined on the IL TOP 700.

Blood samples ( $n = 33$ ) were collected at random time points from 31 patients receiving rivaroxaban treatment for a minimum of 2 weeks. Fourteen results were obtained during 15 mg twice daily dosing and 19 during 20 mg once daily dosing. 19 blood samples were taken around the peak plasma concentration (1.0–5.5 h), 13 during trough periods (12–30 h) and for one patient, the sampling time was uncertain. The anti-Xa rivaroxaban concentrations during peak hours were marginally higher than was expected, with a median of 280 ng/ml (range 168–458). The trough levels were as expected, with a median of 57 ng/ml (range 11–215). There

# Adult T-cell leukemia cells are characterized by abnormalities of *Helios* expression that promote T cell growth

Satomi Asanuma,<sup>1</sup> Makoto Yamagishi,<sup>1</sup> Katsuaki Kawanami,<sup>1</sup> Kazumi Nakano,<sup>1</sup> Aiko Sato-Otsubo,<sup>2</sup> Satsuki Muto,<sup>2</sup> Masashi Sanada,<sup>2</sup> Tadanori Yamochi,<sup>1</sup> Seiichiro Kobayashi,<sup>3</sup> Atae Utsunomiya,<sup>4</sup> Masako Iwanaga,<sup>5</sup> Kazunari Yamaguchi,<sup>6</sup> Kaoru Uchimarui,<sup>3</sup> Seishi Ogawa<sup>2</sup> and Toshiki Watanabe<sup>1,7</sup>

<sup>1</sup>Graduate School of Frontier Sciences, The University of Tokyo; <sup>2</sup>Cancer Genomics Project, Graduate School of Medicine, The University of Tokyo; <sup>3</sup>Institute of Medical Science, The University of Tokyo, Tokyo; <sup>4</sup>Department of Hematology, Imamura Bun-in Hospital, Kagoshima; <sup>5</sup>Graduate School of Public Health, Teikyo University; <sup>6</sup>Department of Safety Research on Blood and Biological Products, National Institute of Infectious Diseases, Tokyo, Japan

(Received December 27, 2012/Revised April 11, 2013/Accepted April 15, 2013/Accepted manuscript online April 18, 2013/Article first published online May 19, 2013)

Molecular abnormalities involved in the multistep leukemogenesis of adult T-cell leukemia (ATL) remain to be clarified. Based on our integrated database, we focused on the expression patterns and levels of Ikaros family genes, *Ikaros*, *Helios*, and *Aiolos*, in ATL patients and HTLV-1 carriers. The results revealed profound deregulation of *Helios* expression, a pivotal regulator in the control of T-cell differentiation and activation. The majority of ATL samples (32/37 cases) showed abnormal splicing of *Helios* expression, and four cases did not express *Helios*. In addition, novel genomic loss in *Helios* locus was observed in 17/168 cases. We identified four ATL-specific short *Helios* isoforms and revealed their dominant-negative function. Ectopic expression of ATL-type *Helios* isoform as well as knockdown of normal *Helios* or *Ikaros* promoted T-cell growth. Global mRNA profiling and pathway analysis showed activation of several signaling pathways important for lymphocyte proliferation and survival. These data provide new insights into the molecular involvement of *Helios* function in the leukemogenesis and phenotype of ATL cells, indicating that *Helios* deregulation is one of the novel molecular hallmarks of ATL. (*Cancer Sci* 2013; 104: 1097–1106)

Adult T-cell leukemia (ATL) is a highly aggressive malignancy of mature CD4<sup>+</sup> T cells and is caused by HTLV-1. After HTLV-1 infection, ATL is thought to develop following a multitude of events, including both genetic and epigenetic changes in the cells. Although many aspects of HTLV-1 biology have been elucidated, the detailed molecular mechanism of ATL leukemogenesis remains largely unknown.<sup>(1,2)</sup> Therefore, to precisely define the comprehensive abnormalities associated with ATL leukemogenesis, we previously carried out global mRNA and miRNA profiling of ATL cells derived from a large number of patients.<sup>(3,4)</sup> In this study, we focused on Ikaros family genes, especially *Helios*, on the basis of our integrated profiling of expression and gene copy number in ATL cells, which revealed the deregulated expression of this family of genes and genomic loss of *Helios* locus.

Ikaros family genes are specifically expressed in the hematopoietic system and play a vital role in regulation of lymphoid development and differentiation.<sup>(5–11)</sup> In addition, they are known to function as tumor suppressors during leukemogenesis according to several genetic studies carried out in mouse models.<sup>(12–15)</sup> Recently, many studies reported the deregulated splicing of Ikaros and the deletion of *Ikaros* locus in several human leukemias.<sup>(16–23)</sup> These abnormalities are associated with poor prognoses.<sup>(24–27)</sup> *Helios* is mainly expressed in the T-cell lineage.<sup>(10,11)</sup> Genomic changes and abnormal expression of *Helios* are also observed in some

patients with T-cell malignancies.<sup>(18,28–31)</sup> However, in contrast to Ikaros, the substantial impact of aberrant *Helios* expression remains to be elucidated because of the absence of functional information, including the target genes of *Helios*.

In this study, we carried out a detailed expression analysis of Ikaros family genes in a large panel of clinical samples from ATL patients and HTLV-1 carriers and consequently identified a novel molecular characteristic, that is, abnormal splicing of *Helios* and loss of expression, which seems to be a significant key factor in leukemogenesis affecting the regulation of T-cell proliferation.

## Materials and Methods

**Cell lines and clinical samples.** HeLa and 293T cells were cultivated in DMEM supplemented with 10% FCS. Human leukemic T cells, Jurkat, Molt-4, and CEM, ATL-derived, MT-1 and TL-Om1, and HTLV-1-infected MT-2 and Hut-102 cell lines were all maintained in RPMI-1640 with 10% FCS. The PBMCs from ATL patients of four clinical subtypes<sup>(32)</sup> and healthy volunteers were a part of those collected with informed consent as a collaborative project of the Joint Study on Prognostic Factors of ATL Development. The project was approved by the Institute of Medical Sciences, University of Tokyo Human Genome Research Ethics Committee (Tokyo, Japan). Clinical information of ATL individuals is provided in Table S1.

**RNA isolation and RT-PCR analysis.** The preparation of total RNA and synthesis of the first strand of cDNA were described previously.<sup>(3)</sup> The mRNAs of Ikaros family genes were examined by PCR with Platinum Taq DNA Polymerase High Fidelity (Invitrogen, Carlsbad, CA, USA). The PCR products were sequenced by automated DNA sequencer. Nested PCR amplification was carried out with diluted full-length PCR products by Accuprime Taq DNA polymerase High Fidelity (Invitrogen). Quantitative PCR was carried out as previously described.<sup>(3)</sup> The specific primer sets for each PCR are described in Table S2.

**Immunoblot analysis.** Cells were collected, washed with PBS, and lysed with RIPA buffer. For immunoprecipitation, cells were lysed with TNE buffer and incubated with specific antibody. Protein samples were then analyzed by immunoblots with specific antibodies: anti-tubulin, anti-Ikaros, and anti-*Helios* antibodies were from Santa Cruz Biotechnology (Santa Cruz, CA, USA). Mouse anti-FLAG antibody (M2) was from Sigma-Aldrich (St. Louis, MO, USA). Rabbit polyclonal anti-HA

<sup>7</sup>To whom correspondence should be addressed.  
E-mail: twnabe@ims.u-tokyo.ac.jp

antibody was from MBL (Nagoya, Japan). Anti-mouse, rabbit, and goat secondary antibodies were from Promega (Fitchburg, WI, USA).

**Immunostaining.** HeLa cells were cultured on coverslip slides and transfected with the indicated expression vectors by Lipofectamine LTX (Invitrogen). At 24 h post transfection, cells were washed three times with PBS, fixed in 4% paraformaldehyde, and permeabilized with 0.1% Triton X-100. Then, cells were stained with primary antibodies (diluted 1:500 to 1:2000). Alexa-488 or 546-conjugated secondary antibodies (Molecular Probes, Life Technologies, Carlsbad, CA, USA) were used for detection of specific targets, and DAPI was used for nuclear staining. Images were acquired by using a Nikon A1 confocal microscope (Nikon, Tokyo, Japan).

**Electrophoretic mobility-shift assay.** Experimental conditions and detail methods were previously reported.<sup>(3)</sup> For evaluation of DNA binding activity, 3–5 µg nuclear extracts from each transfectant were used per each lane of electrophoresis. The oligonucleotide sequences used as a probe are provided in Table S2.

**Luciferase assay.** The pGL4.10-firefly vector (Promega) containing *Hes1* promoter was used as a reporter vector and RSV-renilla vector was used as a control vector. HeLa cells were transiently transfected with these reporters and each Ikaros or/and Helios expression vector by Lipofectamine 2000 reagent (Invitrogen). The luciferase activities were quantified by the Dual-Luciferase Reporter Assay System (Promega) at 24 h post-transfection.

**Retroviral construction and transduction.** The FLAG-Hel-5 cDNA sequence was subcloned into retrovirus vector pRX-puro. Stable cell populations expressing Hel-5 were selected by puromycin. The shRNA-expressing retroviral vectors and virus production procedures have been established.<sup>(3)</sup> The shRNA sequences are listed in Table S2. Stable cell populations were obtained by puromycin or G418 selection.

**Proliferation assays.** Cells ( $0.5$  or  $1.0 \times 10^4$ ) were plated in 96-well plates with media supplemented with 10% or 0.2% FCS. The cell numbers were evaluated for 4 days by Cell Counting Kit-8 (Dojindo, Kumamoto, Japan). The averages of at least three independent experiments are shown.

**Gene expression microarray analyses.** Gene expression microarray used the  $4 \times 44\text{K}$  Whole Human Genome Oligo Microarray (Agilent Technologies, Santa Clara, CA, USA); detailed methods were previously reported.<sup>(3)</sup> Coordinates have been deposited in the Gene Expression Omnibus database with accession numbers GSE33615 (gene expression microarray), GSE33602 (copy number analyses), and GSE41796 (Jurkat models).

## Results

### Abnormal expression of short Helios transcripts in primary ATL cells.

To characterize the gene expression signature in primary ATL cells, we previously carried out mRNA microarray analyses on a large number of samples. The comprehensive survey unveiled deregulated expression of Ikaros family genes; transcription levels of Ikaros and Aiolos were downregulated in ATL samples, whereas Helios was upregulated (Fig. S1). Thus,

we examined the detailed expression patterns and levels of Ikaros family members in PBMCs derived from a panel of ATL patients and HTLV-1 carriers (Fig. 1a). Compared with control PBMCs from normal volunteers (Fig. 1b), the expression levels of Ikaros and Aiolos seemed to be downregulated in ATL samples, consistent with our microarray results. However, there were obvious abnormalities in the expression patterns of Helios. The main isoform of Helios was changed from full-length Hel-1 to Hel-2, which lacks exon 3 that contains the first N-terminal zinc finger in the DNA-binding domain. In addition, four ATL-specific Helios short transcripts were identified (Fig. 1c). Among them, Hel-5 and Hel-6 have been reported to be expressed in ATL.<sup>29</sup> We also identified two novel variants, Hel-v1 that lacks exons 3 and 4 and Hel-v2 that lacks exons 2, 3, and 6. These abnormal Helios variants were also expressed in the samples of high-risk HTLV-1 carriers, who subsequently developed ATL in the next few years. Furthermore, nested PCR revealed that Hel-5 or Hel-6 were expressed in a majority of ATL samples (17/22 acute cases, 10/10 chronic cases, and 5/5 smoldering cases; total, 32/37 cases) (Fig. 1d, upper panels), whereas Hel-v1 was expressed only in limited cases of ATL (Fig. 1d, lower panels). In four cases, Helios was not expressed. Collectively, our mRNA analysis showed that Helios expression was generally deregulated in ATL cells.

### Genomic abnormalities at the *Helios* locus in primary ATL cells.

To investigate the *Helios* locus in ATL, we retrieved data from our gene copy number analysis<sup>(3)</sup> and found that specific genomic deletion was accumulated at the *Helios* locus in ATL samples (17/168 cases, Fig. 2). All 17 cases were aggressive-type ATL (12/17 lymphoma types and 5/17 acute types). Furthermore, we found that two acute ATL cases in Figure 1(a) (#9 and #14), which showed severely deregulated or lost Helios expression, had a genomic deletion of the *Helios* locus.

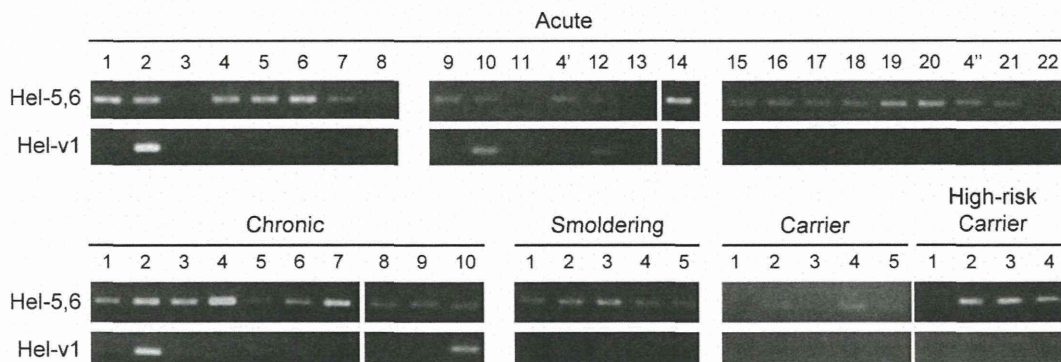
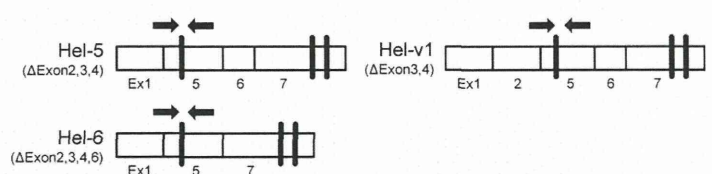
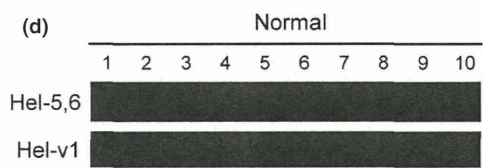
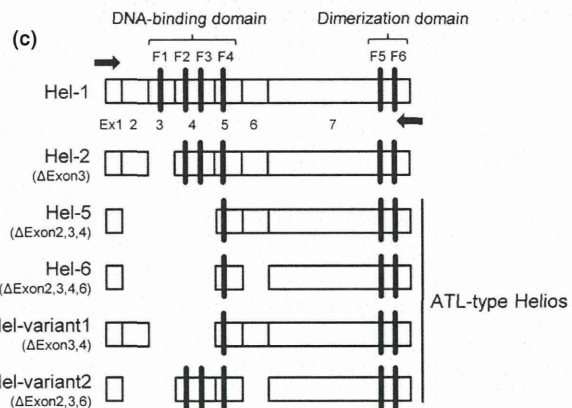
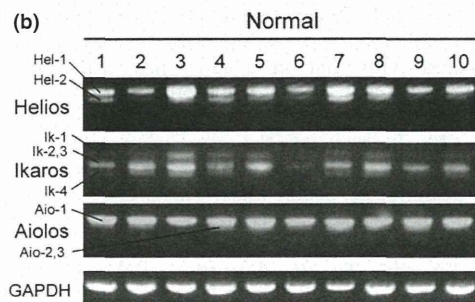
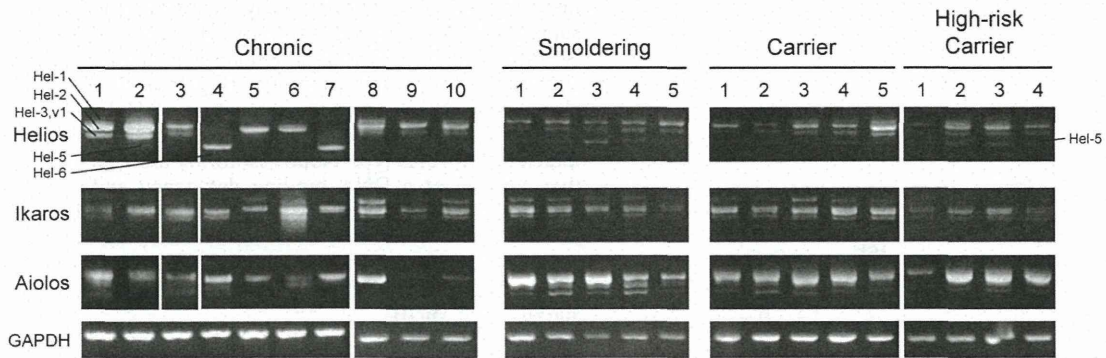
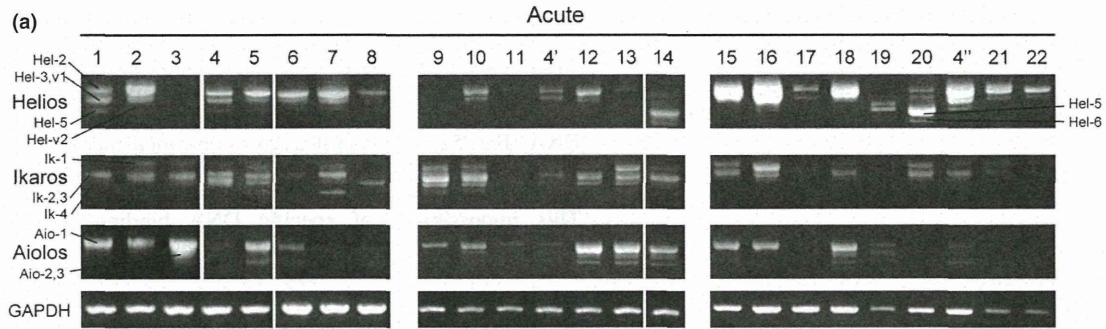
### Dimerization ability of ATL-type Helios isoforms with wild-type Helios or Ikaros.

Consistent with a previously published report,<sup>(33)</sup> co-immunoprecipitation analyses confirmed that wild-type Hel-1 formed homodimers with themselves and heterodimers with wild-type Ikaros (Ik-1) protein (Fig. 3a, top panel, lane 1 and lane 4). In contrast, the dimerization activity of another artificial Helios mutant (Hel-ΔC), which lacks the dimerization domain at the C-terminal region, was dramatically declined (Fig. 3b, top panel, lane 1 and lane 4). We confirmed that all ATL-type Helios proteins could interact with Hel-1 and Ik-1, despite the fact that all of them lack various sets of the N-terminal exons (Fig. 3c–f).

### Cytoplasmic localization of ATL-type Helios isoforms lacking exon 6.

Ectopically expressed Hel-1 and Ik-1 were localized in the nucleus (Fig. 4a, top two panels). Regarding the ATL-type Helios isoforms, we found that Hel-5 and Hel-v1 were localized in the nucleus, whereas Hel-6 and Hel-v2, both of which lack exon 6, were substantially localized in the cytoplasm (Fig. 4a, middle four panels). We also confirmed the cytoplasmic localization of Hel-Δexon 6, which is an artificial Helios mutant lacking only exon 6 (Fig. 4a, bottom panel). Thus, exon 6 appears to be critical for nuclear localization of Helios proteins. Furthermore, defect of exon 6 led to disruption of the

**Fig. 1.** (On the next page) Abnormal expression of Helios mRNA in primary adult T-cell leukemia (ATL) cells. (a) Expression analysis of Ikaros family genes in PBMCs by full-length RT-PCR (Acute,  $n = 22$ ; Chronic,  $n = 10$ ; Smoldering,  $n = 5$ ; HTLV-1 carriers,  $n = 5$ ; High-risk carriers,  $n = 4$ ). To detect and distinguish alternative splicing variants, PCR analyses were carried out with the sense and antisense primer sets designed in the first and final exons of each full-length transcript of Ikaros family genes. Obtained cDNAs were cloned and their sequences were analyzed. The samples acute #4, 4', and 4'' were derived from the same patient, but were studied independently. (b) Expression of Ikaros family genes in PBMCs from normal volunteers ( $n = 10$ ). (c) Schematic representation of Hel-1, Hel-2, and ATL-type Helios isoforms identified in this study. Hel-variant 1 (Hel-v1) and Hel-variant 2 (Hel-v2) are novel isoforms in ATL. Arrows indicate primer locations of full-length PCR for Helios. Ex, exon; F1–F6, functional zinc-finger domains. (d) Nested PCR with specific primer sets, which were designed at exon junction of exon 1–5 or exon 2–5 for detection of Hel-5 and Hel-6 (upper panel), or detection of Hel-v1 (lower panel), respectively. Arrows indicate primer locations.



cellular localization of binding partners. When Hel-6 or Hel-v2 were co-expressed with Hel-1 or Ik-1, they were co-localized in the cytoplasm (Fig. 4b, Fig. S2).

**Dominant-negative function of ATL-type Helios isoforms against wild-type Helios and Ikaros.** We next examined the

functional aspects of these ATL-type Helios isoforms by evaluating their DNA-binding capacities. For EMSA, we used an oligonucleotide probe derived from the promoter region of human *Hes1*, which was a direct target of Ikaros.<sup>(34,35)</sup> Ectopically expressed Hel-1 or Ik-1 could bind human *Hes1* promoter DNA (Fig. 5a). Supershift assays confirmed the binding specificity (Fig. 5b). In contrast, all ATL-type Helios isoforms did not show any specific binding to the *Hes1* promoter (Fig. 5a). This impossibility of specific DNA binding of ATL-type Helios was confirmed with another independent DNA probe, IkBS4<sup>(33,36)</sup> (data not shown). In addition, it was found in co-expression experiments that Hel-5 had antagonistic effects on the DNA binding capacity of Ik-1 in a dose-dependent manner (Fig. 5c). Reporter assays showed that Hel-1 and Ik-1 suppressed *Hes1* promoter activity. However, ATL-type Helios isoforms did not show any suppressive activity, and actually slightly activated the promoter (Fig. 5d). Furthermore, they also inhibited the suppressive function of Hel-1 and Ik-1 in a dose-dependent manner (Fig. 5e, Fig. S3). These data clearly indicate that ATL-type Helios isoforms are functionally defective because of a DNA binding deficiency and act dominant-negatively in transcriptional suppression induced by Hel-1 or Ik-1. We also confirmed that Hel-2, which lacks only exon 3 and is a major isoform in ATL cells, did not possess suppressive activity against *Hes1* promoter in spite of having binding activity (Fig. 5a,d).

**Major ATL-type Helios variant, Hel-5, promotes T cell growth.** Given the tumor-suppressive roles of Ikaros family members,<sup>(12-15)</sup> it was expected that abnormal splicing of Helios could contribute to T cell leukemogenesis. The mRNA level of Helios was significantly downregulated in ATL-related cell lines compared with that in T-cell lines without HTLV-1 (Fig. 6a, Fig. S4). Moreover, Helios protein was not detected in any ATL-derived or HTLV-1-infected cell lines used in this study (Fig. 6b). In contrast, the expression levels of Ikaros mRNA did not show major differences between HTLV-1-infected and uninfected T-cell lines. Those of Aiolos were low in most cell lines irrespective of HTLV-1 infection (Fig. 6a, Fig. S4). Ikaros protein was detected in all T-cell lines used in this study (Fig. 6b). To elucidate the cellular effects of the expression of dominant-negative ATL-type Helios isoforms in T cells, we established stable Jurkat cells expressing Hel-5 (Fig. 6c). A cell proliferation assay confirmed that Hel-5 expression significantly promoted Jurkat cell proliferation

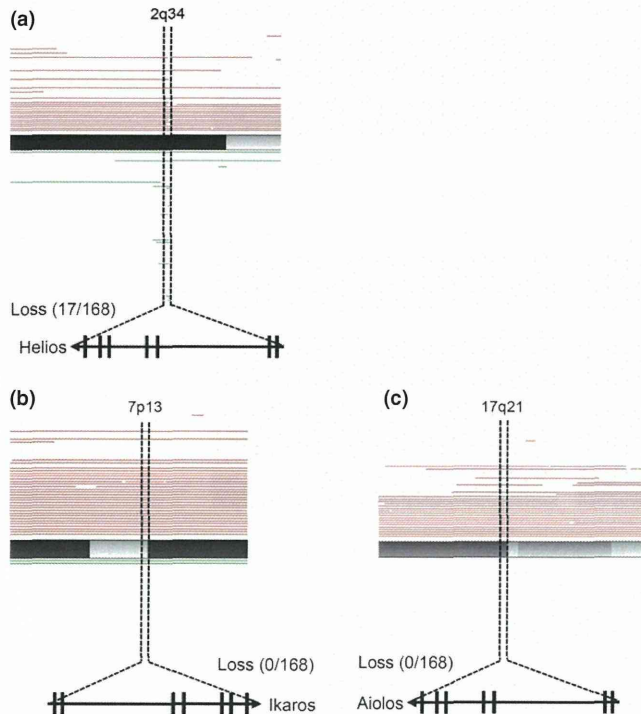


**Fig. 2.** Genetic abnormalities in *Helios* locus in primary adult T-cell leukemia cells. The results of our copy number analyses<sup>(3)</sup> (total number,  $n = 168$ ; acute type,  $n = 35$ ; chronic type,  $n = 41$ ; lymphoma type,  $n = 44$ ; smoldering type,  $n = 10$ ; intermediate,  $n = 1$ ; unknown diagnosis,  $n = 37$ ). Tumor-associated deletion of *Helios* region (17/168) was detected (a). No specific genomic losses were observed in *Ikaros* (b) or *Aiolos* loci (c). Recurrent genetic changes are depicted by horizontal lines based on Copy Number Analyser for GeneChip output of the single nucleotide polymorphism array analysis.

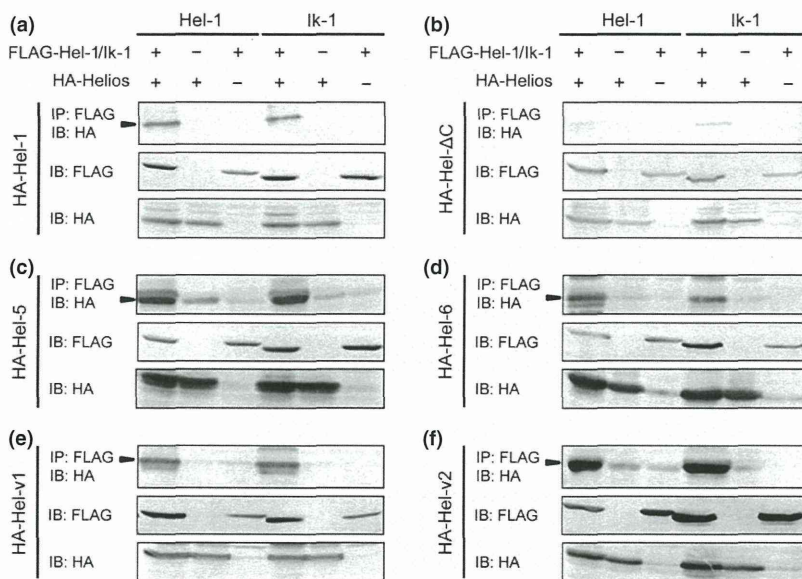


**Fig. 3.** Dimerization ability of adult T-cell leukemia (ATL)-type Helios isoforms. *In vitro* dimerization assays by co-immunoprecipitation between ATL-type Helios and wild-type Helios or Ikaros proteins. 293T cells were transfected with the indicated combination of expression vectors and subjected to co-immunoprecipitation analyses (top panels). Arrowheads indicate the complex of FLAG and HA-tagged proteins. Middle and bottom panels show the input samples. Hel-1 (a) and Hel-ΔC (b) included as positive and negative controls, respectively. ATL-specific isoforms, Hel-5 (c), Hel-6 (d), Hel-v1 (e), and Hel-v2 (f) were tested. IB, immunoblot; IP, immunoprecipitation.

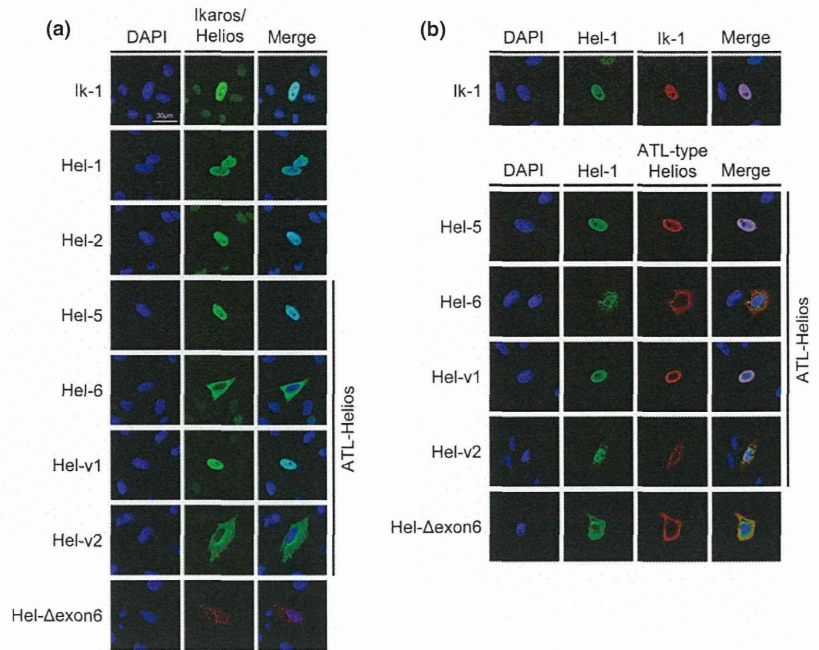


**Fig. 4.** Subcellular localization of adult T-cell leukemia (ATL)-type Helios isoforms. Immunostaining analyses of Helios and Ikaros proteins. HeLa cells were transfected with each individual expression vector (a) or the indicated combination of expression vectors (b). Each protein was visualized with anti-FLAG (green) or anti-HA antibodies (red). Nuclei were detected by DAPI staining (blue). Colocalization between Ik-1 and ATL-type Helios was shown in Fig. S2. Hel-v1, Hel-variant 1; Hel-v2, Hel-variant 2.

(Fig. 6d). To examine whether the cellular effect of Hel-5 was due to its dominant-negative function against Hel-1 and Ik-1, we carried out further knockdown analyses with specific shRNAs (Fig. 6e). The results showed that knockdown of wild-type Helios or Ikaros led to enhanced cell growth (Fig. 6f), which was consistent with the results of enforced Hel-5 expression. These results collectively suggested that counteraction of Ikaros or Helios by dominant-negative isoforms contributed to T cell growth.

**Helios deficiency causes expression of various genes in T cells.** We globally searched mRNA expression changes using microarray analysis of Jurkat cells expressing Hel-5 and those of knocked-down Helios or Ikaros (Fig. 7a,b). The results clearly showed differentially expressed gene sets between the transformants and control cells (Fig. 7c). Furthermore, pathway analysis<sup>(37)</sup> of each upregulated gene set identified activation of several signaling cascades. In particular, we focused on six common pathways identified in both Hel-5 transduced and Helios or Ikaros knocked-down Jurkat cells (Fig. 7d). These pathways are important for various T cell regulations, for example, cell growth, apoptosis resistance, and migration activity. Among these pathways, it has not been reported that the shingosine-1-phosphate (S1P) pathway is regulated by the Ikaros family. We confirmed overexpressed *S1PR1* and *S1PR3*, which are critical receptors for the activation of the S1P pathway, in manipulated Jurkat samples (Fig. 7e).

## Discussion

In the present study, on the basis of the integrated analysis of ATL cells using our biomaterial bank in Japan, we revealed a novel molecular characteristic of ATL cells, which is a profound abnormality in the expression of Helios. The abnormal alternative splicing and, in some cases, loss of Helios expression appear to be a part of the basis for advantageous cell growth and survival in ATL cells. We also showed the tumor-suppressive function and target genes, as well as pathways of Helios, in mature human T cells.

Characterization of Ikaros family members revealed profound abnormalities in Helios expression in ATL cells: (i)

biased and increased expression of alternatively spliced variants; (ii) suppression of Hel-1 expression; (iii) lack of Helios expression in some cases; and (iv) frequent genomic defects of the *Helios* locus. Our results also revealed that alternatively spliced Helios variants are expressed in PBMCs of HTLV-1 carriers, suggesting that the abnormal splicing of Helios may occur in HTLV-1-infected cells at the carrier state until progression to leukemia development. However, the genomic deletions appear to be one of the important genetic events during the latter stages of leukemia development, as they were observed only in aggressive subtypes of ATL.

The structural characteristics of the ATL-type Helios variants involve a selective lack of one or more zinc fingers in the N-terminal domain. The results of this study indicated that these variant proteins lost DNA binding activity, whereas the capacity of dimerization was preserved. Therefore, these variant proteins hindered transcriptional activities of Ikaros family proteins, showing dominant-negative effects. In addition, a part of ATL-type Helios isoform, which lacks exon 6, is linked to abnormal localization of wild-type Helios and Ikaros. We confirmed that Helios isoforms lacking exon 6 were overexpressed in primary ATL cells (Fig. S5). Interestingly, Hel-2 has reduced transcriptional suppressive activity compared with Hel-1, although it can bind to the target sequence as well as Hel-1. This is similar to a previous report,<sup>(36)</sup> which noted that the activity of mouse Ik-2 protein for the reporter gene was remarkably lower than that of Ik-1, whereas the binding affinities of Ik-1 and Ik-2 were similar. The exon 3 skip occurred more frequently in ATL cells, compared to PBMCs from normal volunteers (Fig. S6). These results collectively indicate that all abnormalities of Helios expression, including loss of or decreased Hel-1 expression and upregulated Hel-2 and ATL-type Helios, result in abrogation of Ikaros family functions in ATL cells.

We also confirmed that *Hes1*, a target gene of the Notch pathway, is one of the targets of Helios as well as Ikaros.<sup>(34,35)</sup> A recent study reported that activated Notch signaling may be important to ATL pathogenesis and that *Hes1* is upregulated in ATL cells.<sup>(38)</sup> Thus, we examined expression levels of *Hes1* mRNA by quantitative RT-PCR and confirmed the

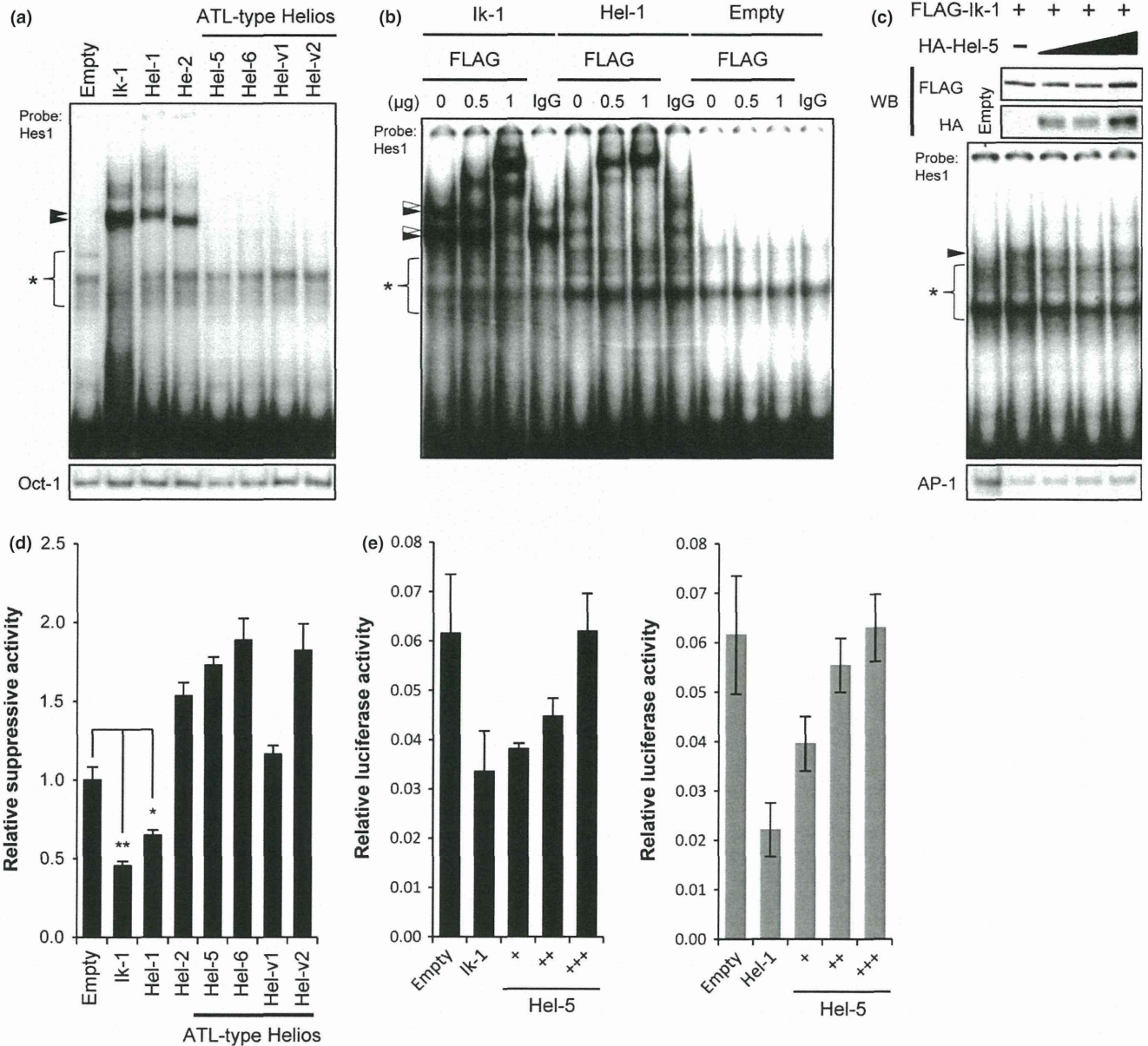


**Fig. 5.** Dominant-negative function of adult T-cell leukemia (ATL)-type Helios isoforms. (a) DNA-binding activities of wild-type Helios or Ikaros and ATL-type Helios proteins. Each FLAG-tagged Helios or Ikaros isoforms were ectopically expressed in 293T cells and their nuclear extracts were subjected to EMSA with a [ $\gamma$ - $^{32}$ P]-labeled *Hes1* promoter probe. Oct-1 probe was used as an internal control. Arrowheads indicate Helios or Ikaros complexes. \*Non-specific bands. Hel-v1, Hel-variant 1; Hel-v2, Hel-variant 2. (b) Results of supershift assays. Anti-FLAG (0, 0.5, 1  $\mu$ g) or control IgG (1  $\mu$ g) antibodies were added to each nuclear extract prior to electrophoresis. The black and white arrowheads indicate the supershifted bands of Ik-1 and Hel-1, respectively. (c) Antagonistic effects of Hel-5 on DNA-binding of Ik-1 tested by EMSA. The molar ratios of Ik-1 to Hel-5 plasmids are 1:1, 1:4, and 1:8. Expression levels of FLAG-Ik-1 and HA-Hel-5 were assessed by immunoblotting. The arrowheads indicate the Ik-1 specific band. AP-1 probe was used as an internal control. WB, western blot. (d) Transcriptional suppression activities of various Helios or Ikaros isoforms tested by *Hes1* promoter-luciferase reporter systems ( $n = 3$ , mean  $\pm$  SD). Basal *Hes1* promoter activity was defined as firefly/renilla ratio, and suppression activities of Helios or Ikaros are relatively presented. Statistical significance was evaluated by unpaired Student's *t*-test (\* $P < 0.05$ ; \*\* $P < 0.01$ ). (e) Inhibitory function of Hel-5 against Ik-1 and Hel-1 tested by *Hes1* promoter assay ( $n = 3$ , mean  $\pm$  SD). The molar ratios of Ik-1 or Hel-1 to Hel-5 plasmids are 1:1, 1:2, and 1:3. Relative luciferase activities were defined as firefly/renilla ratio.

upregulation in our ATL samples (Fig. S7). *Hes1* has been reported to directly promote cell proliferation through the transcriptional repression of p27kip1.<sup>(39)</sup> Taken together, our results suggest a possibility that abnormalities in Helios expression are one of the causes of *Hes1* activation, which may be one of the genetic events involved in ATL leukemogenesis.

Our results show that the Hel-5 variant may have an oncogenic role, whereas the wild-type Helios, Hel-1, shows

tumor suppressor-like activity. These findings are consistent with previous findings in mice.<sup>(15)</sup> Furthermore, our description of expression profiles of stable cells followed by pathway analyses showed activation of several important pathways in lymphocytes for the regulation of proliferation, survival, and others. In particular, we discovered novel molecular cross-talk between the Ikaros family and the S1P pathway. The S1P-S1PR1 axis is known to play important

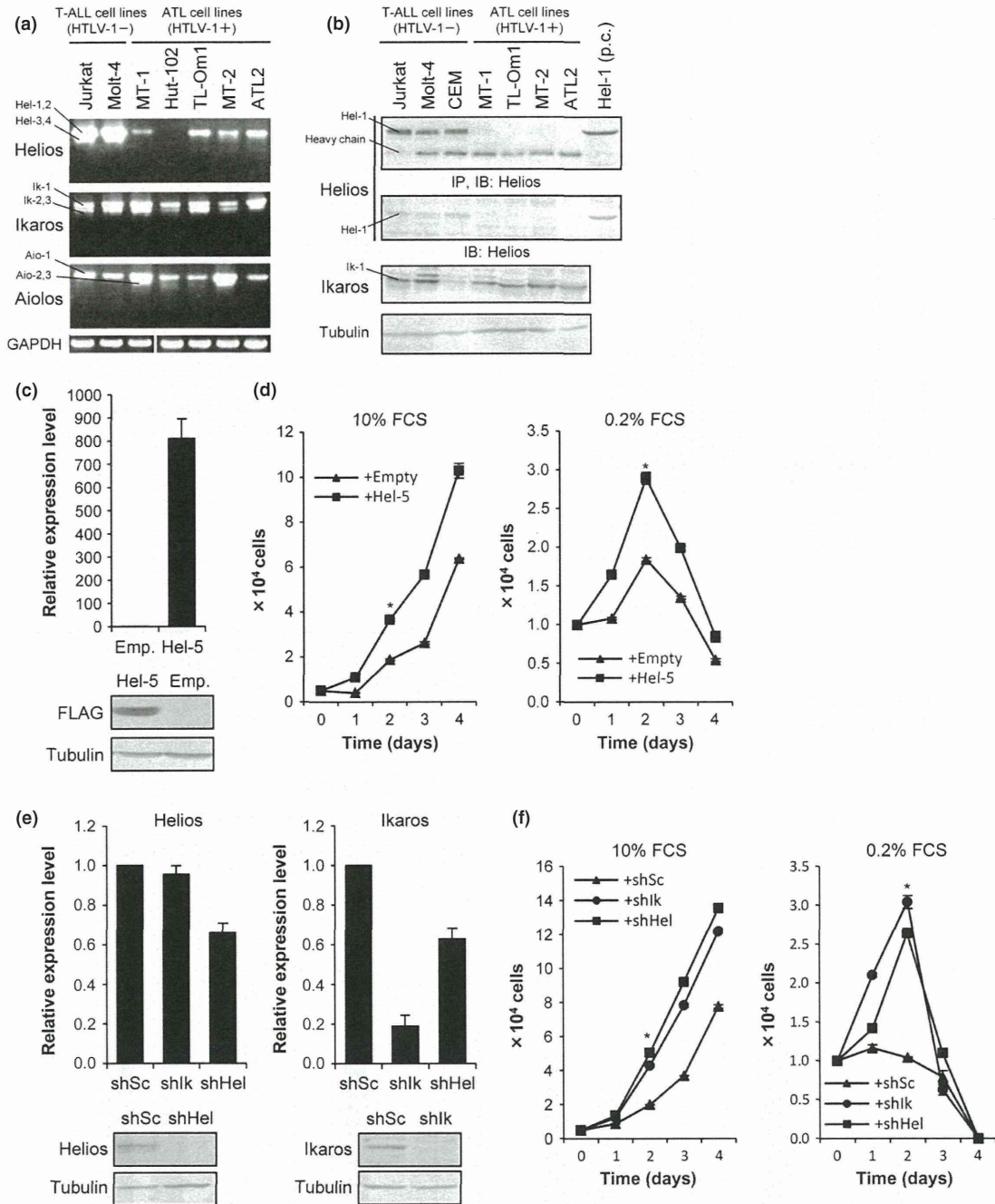


**Fig. 6.** Hel-5 functions in T cell growth and survival. (a) Expression patterns and levels of Ikaros family genes in various cell lines examined by RT-PCR. ATL, adult T-cell leukemia; T-ALL, acute T lymphoblastic leukemia. (b) Results of immunoblotting analyses of the immunoprecipitants (top panel) and cell lysates (lower panels). Positive control (p.c.), Hel-1 transfectant. IB, immunoblot; IP, immunoprecipitant. (c) Establishment of Jurkat cells stably expressing Hel-5. The Hel-5 level was quantified by quantitative RT-PCR (top,  $n = 3$ , mean  $\pm$  SD) and immunoblotting (bottom). (d) Cell proliferation analysis of control cells ( $\blacktriangle$ ) and Hel-5-expressing Jurkat cells ( $\blacksquare$ ) under two FCS conditions ( $n = 3$ , mean  $\pm$  SD). Statistical significance was observed ( $*P < 0.01$ , Student's  $t$ -test). (e) Knockdown analyses of Helios or Ikaros in Jurkat cells. The Helios and Ikaros levels were evaluated by quantitative RT-PCR (top,  $n = 3$ , mean  $\pm$  SD) and immunoblotting (bottom), respectively. (f) Cell proliferation curves of scrambled shRNA (shSc) cells ( $\blacktriangle$ ), shIkaros (shIk) cells ( $\bullet$ ), and shHelios (shHel) cells ( $\blacksquare$ ) were examined in two FBS conditions ( $n = 3$ , mean  $\pm$  SD;  $*P < 0.01$ ).

roles in regulation of the immune system, apoptosis, cell cycle, and migration of lymphocytes.<sup>(40-42)</sup> Recently, activation of the SIP pathway in various diseases, including leukemia, has been reported, and the therapeutic potential of S1PR1 inhibitors was suggested.<sup>(42)</sup> Studies of functional roles of SIP pathway activation in ATL cells are now underway in our laboratory.

In conclusion, our present study revealed a novel aspect of molecular abnormalities in ATL cells: a profound deregulation in Helios expression, which appears to play an important role in T-cell proliferation. Our experimental approaches also imply that, in addition to genetic and epigenetic abnormalities, ATL shows abnormal splicing, which has been observed in various human diseases including cancers.<sup>(43-45)</sup>